OPTIMIZED DYNAMIC TRANSLINEAR IMPLEMENTATION OF THE GAUSSIAN WAVELET TRANSFORM

Sandro A. P. Haddad[1], Nanko Verwaal[1], Richard Houben[2] and Wouter A. Serdijn[1]

[1]Electronics Research Laboratory, Faculty of Electrical Engineer, Mathematics and Computer Science,
Delft University of Technology
Mekelweg 4, 2628 CD Delft, The Netherlands
Email:{s.haddad,w.a.serdijn}@ewi.tudelft.nl

[2]Bakken Research Center
Medtronic
Endepolsdomein 5, 6229 GW Maastricht,
The Netherlands
Email: richard.houben@medtronic.com

ABSTRACT

This paper presents an analog implementation of the Wavelet transform (WT) in an ultra low power environment, using the dynamic translinear (DTL) circuit technique. The circuit consists of an analog filter whose impulse response is the first derivative of a Gaussian. A convenient method to provide the transfer function of the filter is given by the Padé approximation. In order to fulfill the low-power requirement, the filter's state space description is optimized with respect to dynamic range. Finally, the DTL principle is applied to implement the state space filter. Simulations indicate a good approximation of the Wavelet Transform.

Keywords – Wavelet transform, dynamic translinear circuits, ECG characterization, analog electronics, Padé approximation.

1. INTRODUCTION

This paper presents an analog implementation of the wavelet transform with a Gaussian wavelet in an ultra low power environment, using the dynamic translinear circuit technique. The wavelet transform is a merited technique for analysis of non-stationary signals, like cardiac signals. Being a multiscale analysis technique, it offers the possibility of selective noise filtering and reliable parameter estimation. Monitoring and recording in current cardiology practice, which is *in vitro*, employs the discrete wavelet transform, implemented in a digital signal processor. Low power analog realization of the continuous wavelet transform enables its application *in vivo*, e.g. pacemakers and IECG recorders. In these applications, the wavelet transform provides a means to extremely reliable QRS-detection and efficient data storage [1].

The first step of the implementation is the approximation of the ideal transfer function of the filter, the Laplace transform of the gaussian wavelet, by a fifth order rational transfer function, using the Padé approximation. The resulting wavelet has a time-frequency resolution which is better than that of an alternative fifth order approximation [2] and close to the theoretical minimum of ½. Second, the filter's state space description is optimized with respect to dynamic range, using the method proposed by Rocha [3]. Compared to a straightforward implementation, the dynamic range of the optimized state space description has increased by approximately 20 dB. Finally, the individual wavelet transform scales have been implemented, using a hierarchically structured dynamic translinear circuit, following the synthesis method proposed by Roberts [4].

Section 2 deals with the Padé approximation to find the transfer function, which describes the filter. In Section 3, the optimization procedure is applied. Next, Section 4 describes the circuit design. Some results provided by simulations are shown in Section 5. Finally, Section 6 presents the conclusions.

2. APPROXIMATION OF THE MOTHER WAVELET

2.1. Choice of the mother wavelet

The continuous time wavelet transform (WT) of a signal $x(t)$ is described as:

$$\Psi_x(a,\tau) = \frac{1}{\sqrt{|a|}} \int_{-\infty}^{\infty} x(t)\psi^*\left(\frac{t-\tau}{a}\right)dt . \qquad (1)$$

$\psi(t)$ is called the 'template' of the WT or also the 'mother wavelet'. In general, the wavelet transform can be applied using a wide variety of mother wavelets. In many biomedical research applications, the first order derivative of the Gaussian function is a favorite mother wavelet [1]:

$$\psi(t) = -2\sqrt[4]{\tfrac{2}{\pi}} \cdot t \cdot \exp\left(-t^2\right) \qquad (2)$$

There are two reasons for the use of the Gaussian wavelet. The main reason is that the product of its time resolution and its frequency resolution takes the theoretical minimum value of ½ [5]. Consequently, a wavelet transform with the gaussian wavelet gives the most accurate estimation of frequency components localized in time [6]. The second reason can be seen from detection theory. A certain waveform in a signal with additive gaussian white noise will be detected optimally if the impulse response of the filter is the time-reverse of that waveform [7]. Applying this to the case of ECG analysis, we denote some similarity between the contents of the ECG, particularly the QRS complex, and the gaussian wavelet. Therefore the first order derivative of the gaussian function is a good approximation to the 'matched' filter.

2.2. Padé Approximant

The Padé approximation is an approximation that concentrates around one point of the function that needs to be approximated. The reason to apply the Padé approximation is that it immediately yields a rational expression, which is suitable for

implementation. In the Padé approximation, the coefficients of the approximating rational expression are computed from the Taylor coefficients of the Laplace Transform of $\psi(t)$.

Suppose we have the truncated Taylor series expansion of a general function *F(s)* around some point, e.g., $s = 0$:

$$F(s) = c_0 + c_1 s + \cdots + c_k s^k + O\left(s^{k+1}\right) \tag{3}$$

The constants c_0 to c_k are called the Taylor coefficients. Unfortunately, *F(s)* is not a suitable expression to build a filter, since it has only zeros. Then, the Padé approximation $\hat{F}(s)$ of a function $F(s)$ is given by:

$$\hat{F}_{[m/n]}(s) = \frac{P(s)}{Q(s)} = \frac{p_0 + p_1 s + \cdots + p_m s^m}{q_0 + q_1 s + \cdots + q_n s^n} \tag{4}$$

where the coefficients of $Q(s)$ are:

$$\underline{q} \in Nullspace\left(\begin{bmatrix} c_{m+1} & \cdots & c_0 & 0 \\ & & & c_0 \\ \vdots & & & \vdots \\ c_{m+n} & \cdots & & c_m \end{bmatrix}\right) \tag{5}$$

with $q_n = 1$. The coefficients of $P(s)$ are:

$$\underline{p} = \begin{bmatrix} p_0 \\ \vdots \\ p_m \end{bmatrix} = \begin{bmatrix} c_0 & 0 & \cdots & 0 \\ c_1 & c_0 & \ddots & \vdots \\ \vdots & c_1 & \ddots & 0 \\ \vdots & \vdots & \ddots & c_0 \\ \vdots & \vdots & & c_1 \\ \vdots & \vdots & & \vdots \\ c_m & c_{m-1} & \cdots & c_{m-n} \end{bmatrix} \cdot \underline{q} \tag{6}$$

with $c_k = 0$ for $k < 0$.

Then, if the approximation rational function has a numerator of order m and a denominator of order n, the original function can be approximated up to order $m+n$.

The main advantage of the Padé approximation is its computational simplicity and its general applicability. Therefore, it can easily be applied to other filters with a prescribed impulse response, for example to build WT filters with alternative mother wavelets.

On the basis of the time-frequency resolution product, we think that the [3/5] Padé approximation is a suitable candidate for implementation. It is almost symmetrical, it has almost no overshoot and its time-frequency resolution product is only 5% above the Heisenberg limit of ½, while its order 5, is reasonable. We conclude the section by giving the transfer function of this approximation, which will be the basis for implementation in the next section:

$$\hat{H}_{a,[3/5]}(s) = \frac{92.4s - 18.3s^2 + 5.75s^3}{52.3 + 94.5s + 74.8s^2 + 33.0s^3 + 8.33s^4 + s^5} \tag{7}$$

3. DYNAMIC RANGE OPTIMIZATION

Departing from the transfer function derived in Section 2, we generate a state space description of the filter, which is optimized with respect to the Dynamic Range. In [3] a method to optimize the state space description of a dynamical system is presented, based on the observability and controllability gramians. The resulting system has, under certain conditions, the maximum dynamic range which is achievable, given the total amount of capacitance. We shall follow his approach and apply the method to our filter.

The common form of the state space description is:

$$\begin{aligned} \frac{d}{dt}x(t) &= Ax(t) + Bu(t) \\ y(t) &= Cx(t) + Du(t) \end{aligned} \tag{8}$$

The input and output signals of the system are $u(t)$ and $y(t)$, respectively. The vector variable $x(t)$ represents the state of the system. The entries of A, B, C and D are derived directly from the coefficients of the transfer function.

The controllability and observability gramians are derived from the state space description. The definition of the controllability gramian is, related to the system matrices A and B:

$$K = \int_0^\infty e^{At} B B^T e^{A^T t} dt \tag{9}$$

The observability gramian is, related to the system matrices A and C:

$$W = \int_0^\infty e^{A^T t} C^T C e^{At} dt \tag{10}$$

In practice, both gramians are computed by solving a Lyapunov matrix equation.

Finally, we will give the objective functional that will be used to evaluate the gain in dynamic range. Under the assumption that all noise sources in the circuit can be transformed to the integrator inputs and that the equivalent noise sources at the integrator inputs have the same level for all integrators, the absolute dynamic range is expressed as [3] :

$$DR = \frac{\left(\frac{M}{\delta(p)}\right)^2 Tr(KQ)}{\max_i k_{ii}} \frac{1}{\gamma \sum_i \frac{\alpha_i}{C_i} w_{ii}} \tag{11}$$

where M is the maximum integrator representation capacity (clipping level), $\delta(p)$ is a nonlinear function relating undesirable high signal levels at the integrators to the chance p that these signal levels occur, Q is called the state weighting matrix and is defined $Q = C^T C$, $Tr(\bullet)$ is the trace operator (sum of main diagonal elements), k_{ii} and w_{ii} are the main diagonal elements of K and W respectively, $\alpha_i = \sum_j |A_{ij}|$ is the absolute sum of the elements on the i-th row of A, C_i is the capacitance accommodated in integrator i and, finally, γ is a constant representing the integrator noise figure.

Although (11) seems an impressive expression for maximization, it can be shown that M, $\delta(p)$, $Tr(KQ)$ and γ are invariant to similarity transforms. In this paper we are only concerned with the relative improvement of our

optimization procedure, so we will use the following objective functional, according to [3], which will be minimized:

$$F_{DR} = \max_i k_{ii} \sum_i \frac{\alpha_i}{C_i} w_{ii} \tag{12}$$

Hence, in order to maximize the dynamic range of the system, one should minimize the objective functional.

As the dynamic range of a circuit is defined as the ratio between the maximum and the minimum signal level that it can process, optimization of the dynamic range is equivalent to the simultaneous maximization of the (distortion-less) output swing and the minimization of the overall noise contribution. In [3], Rocha gives a geometric interpretation of the optimization of the dynamic range. He relates the output swing via the controllability gramian to the space of 'occurring' state space vectors. Under the assumption of a random input signal, the shape of this space generally is a multidimensional ellipsoid. The constraint that each integrator has a maximum representation capacity defines a multidimensional cuboid, which, for a distortionless transfer, should contain the former mentioned ellipsoid completely. As the mean radius of the ellipsoid is equivalent to the maximum output swing, the output swing is maximized when the mean radius of the ellipsoid is maximal. This occurs if and only if the ellipsoid becomes a spheroid. In that case the controllability gramian is a diagonal matrix with equal diagonal entries, which means that all axes of the ellipsoid have equal length. Thus, the first optimization step boils down to a similarity transform, such that the controllability gramian of the new system becomes a diagonal matrix with equal diagonal entries.

In the second step of the optimization procedure, the system is optimized with respect to its noise contribution. Rocha defines another ellipsoid, which describes the noise that is added to the state vector in each direction. While preserving the result of the first optimization step, it is possible to rotate the state space, such that the observability gramian becomes a diagonal matrix as well. In that case, the axes of the noise ellipsoid are aligned with the 'system axes'. Profiting from the well-known fact that the relative noise contribution of an integrator decreases when the capacitance and bias current increase, the capacitance distribution can be matched now to each integrator's noise production. Thus, the optimum capacitance distribution is given by [3]:

$$C_i = \frac{\sqrt{\alpha_i w_{ii} k_{ii}}}{\sum_j \sqrt{\alpha_j w_{jj} k_{jj}}} \tag{13}$$

Finally, compared to a straightforward implementation (e.g. a cascade of biquads), we can reach a maximum gain in Dynamic Range of 19.6dB by optimization. However, the state-space matrices of the dynamic-range-optimal system is generally fully dense and due the complexity of its implementation, we sometimes have to trade off between a less complex implementation and a better dynamic range. For our filter, we opt for the fully optimized state space description.

4. CIRCUIT DESIGN

4.1. Multiple input log-domain integrator

First, the log-domain integrator, which is the basic building block of the filter, will be presented. The multiple input log-domain integrator is shown in Fig.1. The operation of the circuit is as follows. A positive voltage across the base-emitter junction of Q1 causes a collector current, which discharges the capacitance through the collector-base connection. A positive voltage across the base-emitter junction of Q2 causes a collector current, which charges the capacitance via the current mirror on top. The net current flowing into the capacitance is the difference of collector currents from the positive and negative input side. In addition, we implement the state space coefficients (a_{ij} or b_i), by placing constant voltage sources, V_{mp} and V_{mn}, in series with each base-emitter junction. Finally, we propose to subtract a constant number α of each *exp( )* term in order to perform the integration operation for both positive and negative input variables. This is implemented by the transistors Q3 and Q4 and the constant voltages sources V_{bp} and V_{bn}, respectively. An alternative view on subtracting a constant number is defining the operating point. This is basically the same as biasing. However, in contrast to the regular design of linear circuits, we cannot separate the design of the signal processing function and the design of the bias function. Since the circuit is nonlinear and intended to be used in the large signal range, the superposition principle is not valid. Therefore, the biasing function is an integrated part of the signal processing design.

Thus, the current flowing into the capacitance is defined as:

$$i_C = C\frac{dV_C}{dt} = I_S e^{\left(\frac{V_C + V_{mp} - V_{ip}}{V_t}\right)} - I_S e^{\left(\frac{V_C + V_{mn} - V_{in}}{V_t}\right)} + I_S e^{\left(\frac{V_C + V_{bp}}{V_t}\right)} - I_S e^{\left(\frac{V_C + V_{bn}}{V_t}\right)} \tag{14}$$

with

$$V_{mp,mn} = V_t \ln\left(\frac{a_{ij}, b_j}{I_s}\right) \tag{15}$$

$$V_{bp,bn} = \alpha \cdot V_{mp,mn} \tag{16}$$

where a_{ij}, b_j are the multiplication coefficients of the matrix A or matrix B in the state space description. $V_{mp,mn}$ are the positive and negative multiplication voltages respectively. $V_{bp,bn}$ are the positive and negative voltages which implement the biasing function. I_s is the saturation current.

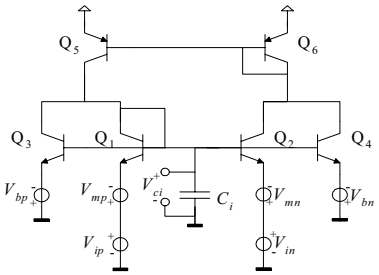

Fig. 1. Log-domain integrator

4.2. Log-domain realization of the state space description

In this subsection, we will design the circuit implementing our wavelet filter, based on the multiple input log-domain integrator. A block schematic of the total filter is drawn in Fig. 2. The A-matrix, B-matrix and C-matrix each have five connections to the capacitances.

Let us start with writing each row of (8) separately

$$\frac{d}{dt}x_i = \sum_{j=1}^{5} \tau^{-1} a_{ij} x_j + b_i u$$
$$y = \sum_{i=1}^{5} c_i x_i \qquad (17)$$

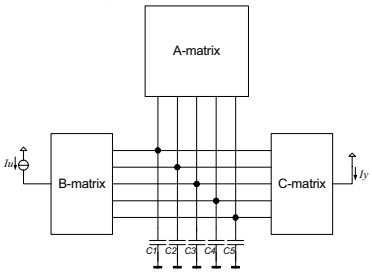

Fig. 2. Block diagram of the complete system

Notice that we introduce the constant τ ($\tau = CV_t$), which represents the time constant of the circuit. We define the five states x_1 to x_5 with an exponential relation to the capacitance voltages V_{C1} to V_{C5}. The input signal u and output signal y are linearly related to the currents I_u and I_y. So the correspondence relation is defined as:

$$i_{ci} = -\sum_{j:a_{ij}>0} |a_{ij}| e^{\left(\frac{V_{ci}-V_j}{V_t}\right)} + \sum_{j:a_{ij}<0} |a_{ij}| e^{\left(\frac{V_{ci}-V_j}{V_t}\right)} + \sum_j a_{ij} e^{\left(\frac{V_{ci}}{V_t}\right)} - b_i C V_t I_u e^{\left(\frac{V_{ci}}{V_t}\right)}$$
$$I_y = \sum_{i=1}^{5} c_i \left(e^{\left(\frac{V_{ci}}{V_t}\right)} - \alpha \right) \qquad (18)$$

We see that the terms of the capacitance current have exactly the same form as the multiple input log domain integrator expression (14) and thus can be implemented in the same way. However, in order to maintain the overall linearity of a log-domain system, a *LOG* stage must be added to the input, while an *EXP* stage is required at the output. The *LOG* and *EXP* stages are shown in Fig.3. By adding a summation stage at the output, we can obtain the expression for output current.

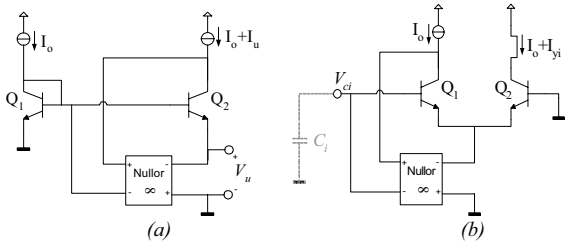

Fig. 3. (a) *LOG* stage (b) *EXP* stage

The nullors can be implemented by a cascade of a common-collector and a common-emitter stage, or, in case of a BiCMOS process, a single common-source stage.

5. SIMULATION RESULTS

To validate the system principle and to check the circuit performance, the whole system has been simulated using models of our in-house bipolar semi-custom IC process, SIC3A [8]. Typical transistor parameters are $f_{T,\mathrm{npn,max}}$ = 15GHz and $\beta_{F,\mathrm{npn}}$ = 150 (smallest emitter size). The circuit has been designed to operate from a 2-V supply voltage.

First, we have set α = 1 and τ = 1ms. The impulse response of the circuit was simulated by applying an input pulse waveform of length 0.1µs and of height 1nA. The acquired output signal is plotted in Fig. 4. The output current presents an offset of approximately 80pA. For illustration we have added the plots of the mathematical impulse response of the original state space filter and the delayed first derivative of the Gaussian.

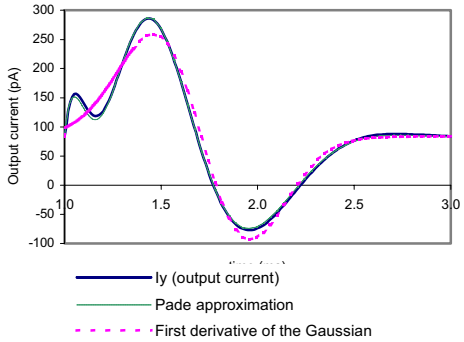

Fig. 4. Simulated Impulse response of the filter

As we can see in Fig. 4, the simulated impulse response differs only slightly from the approximated response, which was acquired directly from the, Padé approximation. We conclude that the coefficients have been implemented successfully.

6. CONCLUSIONS

Our conclusions are threefold: first, Padé approximation in the Laplace domain is an efficient and convenient means to approximate the transfer function of an impulse response specified filter; second, the acquired fifth order approximated gaussian wavelet yields a more accurate wavelet transform; third, dynamic range optimization of a dynamic translinear circuit implementation minimizes the required power consumption of the continuous wavelet transform and makes *in vivo* cardiac applications possible.

REFERENCES

[1] J.S. Sahambi, S.N. Tandon and R.K.P. Bhatt, "Using Wavelet Transform for ECG Characterization," *IEEE Eng. in Medicine and Biology*, pp. 77-83, Jan/Feb. 1997.

[2] S. A. P. Haddad and W. A. Serdijn, "Mapping the Wavelet Transform onto silicon: the Dynamic Translinear approach," *Proceedings IEEE International Symposium Circuits & Systems*, vol. 5, pp. 621-624, May 2002.

[3] D. P. W. M. Rocha., "Optimal Design of Analogue Low-Power Systems, A strongly directional hearing-aid adapter," *PhD thesis*, Delft University of Technology, April 2003.

[4] G. W. Roberts and V. W. Leung, "Design and Analysis of Integrator-based Log-domain Filter Circuits," *Kluwer*, Boston, 2000.

[5] A. Cohen and J. Kovacevic, "Wavelets: the mathematical background," *Proceedings of the IEEE*, vol. 84, no. 4, Apr. 1996.

[6] M. Unser and A. Aldroubi, "A review of wavelets in biomedical applications," *Proceeding of the IEEE*, vol. 84, no. 4, Apr. 1996.

[7] G. A. Baker Jr., "Essentials of Padé Approximants," *Academic Press*, New York, 1975.

[8] W. Straver, "Design Manual – SIC3A", Internal Report, Delft University of Technology, January 1999.